NJC

ROYAL SOCIETY OF CHEMISTRY

PAPER

View Article Online
View Journal | View Issue

Cite this: *New J. Chem.*, 2021, **45**, 13934

Novel PET-pperated rosamine pH-sensor dyes with substitution pattern-tunable pK_a values and temperature sensitivity†

Elina Andresen,[ab] Sebastian Radunz[a] and Ute Resch-Genger *[a]

Received 21st May 2021,
Accepted 3rd July 2021

DOI: 10.1039/d1nj02505h

rsc.li/njc

We present the synthesis and characterization of a family of regioisomerically pure pH-sensitive rosamine fluorophores consisting of xanthene fluorophore cores, which determine the dyes' photophysical properties such as excitation/emission wavelength, fluorescence quantum yield, and fluorescence lifetime, and differently substituted phenol moieties. The hydroxyl substituent of the phenol moiety introduces a pH sensitivity of the dyes' fluorescence exploiting a photoinduced electron transfer (PET), that leads to a protonation-induced switching ON of the rosamine emission. Rational tuning of the pK_a value of the rosamine fluorescence between 4 to 9 is achieved by altering the substitution pattern and degree of bromination of the phenolic subunits. Additionally, a temperature sensitivity of the fluorescence quantum yield is introduced or suppressed based upon the degree of rigidity of the xanthene scaffold.

1 Introduction

Luminescence-based sensing and imaging plays a significant role in the life sciences because it enables the non-invasive and spatially resolved detection, monitoring, and quantification of biomolecular interactions or neutral and ionic targets that have no intrinsic color or luminescence with the aid of specifically designed fluorescent probes.[1–5] Signaling of specific interactions or the presence of a target or analyte is done by spectroscopically measurable changes in the probes' absorption and/or fluorescence properties. The readout parameters include changes in intensity and/or spectral position of the absorption/excitation and emission bands.

Fluorescent probes that undergo reversible spectroscopic changes are often also termed fluorescent (chemical) sensors, while molecules that reveal irreversible changes in their optical properties caused by the breakage of chemical bonds are referred to as chemodosimeters.[6–10]

Of particular interest are fluorescent probes for biologically, health, and corrosion-relevant analytes such as pH.[11–15] Here, photoinduced electron transfer (PET) – based probes which reveal protonation-induced changes in fluorescence quantum yield and lifetime, while the spectral position of their absorption and emission bands is not or only barely affected, are highly desired Such probes consist of a fluorophore moiety and an electronically decoupled protonation side. Protonation-induced spectral changes in absorption and emission together with relatively moderate intensity changes can be realized, if the (de)protonable group is part of the π-electron system of a charge transfer (CT)-operated chromophore. These modifications are caused by changes in the electron density of the (de)protonable group, which affects the light-induced intramolecular CT process.[16–19]

For the design of PET probes, fluorophores like fluoresceins,[20] naphthalimides,[21] BODIPYs[22–24] and aza-BODIPYs,[25] are combined with electron donating (de)protonable moieties with non-bonding electron pairs provided by nitrogen or oxygen atoms. Electronic excitation of these PET probes leads to an electron transfer from the electron rich receptor to the electronically decoupled excited fluorophore promoting fluorescence quenching. Protonation of the donor receptor changes the energetic position of its HOMO, thereby preventing PET and reversibly switching ON the fluorophore's emission.

Xanthene dyes like fluoresceins, rhodamines, and rosamines are particularly attractive fluorophores for the design of fluorescent probes because of their excellent photophysical properties.[26,27] This includes high molar absorption coefficients and high fluorescence quantum yields in the visible or red spectral region as well as a relatively high photostability. Rhodamine fluorophores, which consist of a planar xanthene ring 3,6-disubstituted by in-plane amino groups and a nearby perpendicular 2′-carboxyphenyl ring in position 9 (see Fig. 1A), have been employed in many different probes and sensing applications.[28–31] A previously developed

[a] *Federal Institute for Materials Research and Testing (BAM), Division Biophotonics, Department 1, Richard-Willstaetter-Straße 11, D-12489 Berlin, Germany. E-mail: ute.resch@bam.de*
[b] *Humboldt-Universität zu Berlin, Department of Chemistry, Brook-Taylor-Straße 2, 12489 Berlin, Germany*

† Electronic supplementary information (ESI) available. See DOI: 10.1039/d1nj02505h

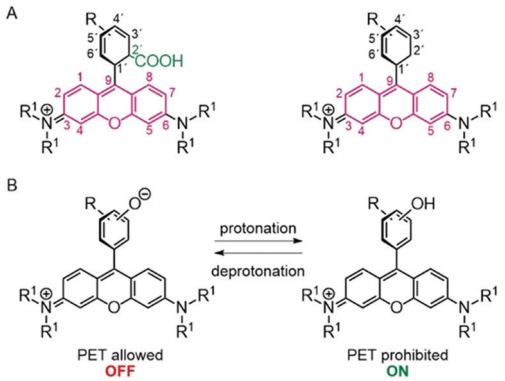

Fig. 1 (A) General structures of rhodamine and rosamine dyes with the xanthene core being highlighted in pink. (B) Mechanism of pH sensing of a rosamine dye *via* intramolecular photoinduced electron trasfer (PET).

strategy to design pH-sensitive rhodamine dyes exploits protonation-induced structural changes, *i.e.*, the switching from the spirocyclic to the ring-open form of certain rhodamine derivatives.[32–41] These so called rhodamine spirolactams (RSLs), which are readily accessible by amidation of the carboxylic group of commercially available rhodamines are colorless and non-fluorescent in their spirocyclic form. Protonation of the amide nitrogen induces the opening of the spirocyclic ring system, yielding the fully conjugated and highly fluorescent rhodamine dye. However, these RSLs reveal a limited pK_a tunability as substituents of different bulkiness on the carboxylic group of rhodamine B or rhodamine 6G can introduce a steric hindrance of the signal-generating ring-opening mechanism.[34,40] This can considerably slow down their response to pH.[39]

Another potentially favorable property of rhodamines bearing sterically non-hindered unbridged dialkylamino substituents can be the sensitivity of their fluorescence intensity or quantum yield to temperature.[42–44] This has been utilized for luminescence-based temperature sensors[42] but could be also disadvantageous for other applications. Only rhodamines with rigidized, *i.e.*, fused cyclic rings on their xanthene nitrogen atoms like rhodamine 101 or rhodamine 6G reveal a temperature-independent fluorescence.

Thus, alternative concepts for designing fluorescent pH-probes utilizing xanthene dyes are of great interest. Rosamines, which are xanthene-type dyes lacking the carboxylic group in the 2′-position (see Fig. 1A), are less well studied, despite their similarly attractive optical properties. Moreover, they can be easily synthesized and isolated as single regioisomers.[45] Hence, they can provide an ideal platform for the rational design of stimuli-responsive fluorophores. So far, only few pH-sensitive rosamine-based probes have been reported that utilize PET.[46–48] These dyes typically consist of a fluorophore and a nitrogen-containing subunit, either a piperazonium group[46] or an amine-containing side chain,[47] located in close proximity to the xanthene core.

To the best of our knowledge, the only series of pH-sensitive rosamine dyes (referred to as rhodamines by the authors) bearing a phenolate group as pH sensitive subunit was reported by Collot's group.[48] These dyes, called H-Rubies, are derived from rhodamine X and possess different pK_a values depending on the substitution pattern of the phenolic subunit. However, these dyes were not systematically spectroscopically assessed and a systematic tuning of their pK_a-was not explored.

Herein, we present a series of novel pH-sensitive rosamine dyes with tuneable pK_a values, introduced by altering the substitution pattern of the phenolic moiety. Tuning of their photophysical properties was achieved by modulation of the xanthene unit. Subsequently, the spectroscopic properties of this new family of sensor dyes and their pH-responsivity are systematically assessed as well as their potential as temperature sensors. To the best of our knowledge, this presents the first example of systematic pK_a-tuning for PET-based phenol-modulated pH-sensitive rosamine-based dyes.

2 Experimental section

2.1 Materials

3-Hydroxybenzaldehyde (≥99%) and *p*-toluenesulfonic acid monohydrate (≥98%) were purchased from Sigma-Aldrich. 8-Hydroxyjulolidine (97%) and *p*-chloranil (97%) were obtained from Alfa Aesar,3-diethyl-aminophenol (98%) was purchased from J&K, and 4-hydroxy-benzaldehyde (≥99%) was obtained from Roth. Propionic acid (99.5%) was purchased from Honeywell and chloroform, and dichloromethane and methanol from Carl Roth GmbH. All chemicals were used without further purification. Brominated hydroxybenzaldehydes were provided by S. Radunz; their synthesis and characterization is described in a previous work.[22] ALUGRAM Xtra SIL G/UV254 plates by Macherey-Nagel were used for thin-layer chromatography. Isolation of products by chromatography was performed with silica from Macherey-Nagel Silica 60 M (0.04–0.063 mm).

2.2 General procedure for rosamine synthesis

To a solution of aldehyde (1 eq.) in propanoic acid 3-diethyl-aminophenol or 8-hydroxyjulolidine (2 eq.) and *p*-TsOH (1 eq.) were added. The solution was protected from light and stirred at 80 °C for 2 h. After cooling to room temperature (rt), chloranil (1.1 eq.) was added to the reaction mixture that was then stirred overnight at rt. The resulting dark purple solution was evaporated to dryness and the crude product was purified by column chromatography on silica gel (DCM/MeOH, 98/2 to 90/10) yielding the desired compound as a purple or violet solid. For detailed synthesis and characterisation of the dyes can be found in the ESI.†

2.3 NMR spectroscopy and mass spectrometry

NMR spectra were recorded on a JEOL Eclipse+ 500 (^{1}H 500 MHz, ^{13}C 126 MHz) and BRUKER AVANCE 700 (^{1}H 700 MHz, ^{13}C 176 MHz) spectrometer at 25 °C. The chemical shifts δ are calibrated on the respective solvent peak as internal standard (^{1}H: $\delta(CD_3OH)$ = 3.31 ppm; ^{13}C: $\delta(CD_3OH)$ = 77.16 ppm). All shifts are reported in in parts per million (ppm) and NMR multiplicities.

2.4 Optical spectroscopy

Absorption measurements were carried out on a calibrated Varian Cary 5000 UV-/VIS-/NIR spectrophotometer with a scan

rate of 600 nm s^{-1} and a slit width of 2 nm using a baseline correction (air/air) and a solvent sample as a reference.

Fluorescence spectra were recorded on a calibrated FLS920 spectrofluorometer from Edinburgh Instruments with an integration time of 0.3 s and slit widths of 6.0 nm of the excitation and emission monochromators. The excitation wavelength was set to 540 nm for dyes **1a–c***, dyes **2a,b** and dye **3** and to 570 nm for dyes **1d** and **2c**, respectively.

All optical measurements were done with 1 cm quartz glass cuvettes from Hellma GmbH.

Fluorescence quantum yields were determined absolutely using a Quantaurus-QY integrating sphere spectrometer C11347-01 from Hamamatsu Photonics K. K. using special long-neck quartz cells provided by the instrument manufacturer. The absorbance of the sample solutions was kept below 0.1 at the excitation wavelength (λ_{ex} = 540 nm). The quantum yield values of the dyes given were obtained by averaging five independent measurements. To determine the fluorescence quantum yield of the protonated species, 5 μl of concentrated HCl (12 M) were added to 3 ml of a 1×10^{-6} M ethanolic solution of the dyes.

The determination of fluorescence lifetimes was carried out with a FLS920 spectrofluorometer from Edinburgh Instruments using a femtosecond supercontinuum laser. The repetition rate was set to 10 MHz. The fluorescence lifetimes were measured for methanolic dye solutions with concentrations of 5×10^{-6} M. The excitation wavelength was set to 540 nm for dyes **1a–c***, dyes **2a**, **b**, and dye **3** and to 570 nm for dyes **1d** and **2c**, respectively. All fluorescence decay curves were measured in 1 cm quartz cuvettes from Hellma GmbH and were evaluated using the software FAST (Edinburgh Instruments) and applying monoexponential fits to obtain the provided fluorescence lifetimes.

pH-titration experiments were carried out with solutions of the dyes in a 1/2 (v/v) mixture of methanol and aqueous buffer (borate-citrate, 25 mM) with dye concentrations of 1×10^{-6} M, thereby also suppressing a possible dye dimerization and self-quenching. The pH values of the used buffer solutions were previously adjusted with a 780 pH meter using a glass electrode from Deutsche METROHM GmbH & Co. KG and were verified with a pH 211 microprocessor pH meter from Hanna Instruments. The 780 pH meter was calibrated in a three-point calibration with standard buffers of pH 10.01, 7.01, and 4.01 (Hanna Instruments) at 25 °C. For the determination of the pK_a-values, 5 μl of the methanolic stock solutions of the dyes (2×10^{-3} M) diluted in 2 ml methanol, were added to 1 ml buffer, resulting in a 1×10^{-6} M dye solution. Successively, defined amounts of concentrated NaOH were added and the absorption and fluorescence emission spectra were collected at the respective pH. pK_a-values were determined from 3 independent samples and measurements applying a sigmoidal curve fit (see ESI,† eqn (S1)).

The temperature dependent fluorescence intensity measurements were performed in triplicate in from the temperature range of 10 °C to 50 °C in 5 °C steps (using equilibration times of 5 min and stirring the solutions in between the measurements). After heating to 50 °C the sample was cooled down to 10 °C and the fluorescence intensity was measured again to confirm the thermal stability of the studied rosamine dyes.

3. Results and discussion

3.1 Design and synthesis of pH-sensitive rosamines with tunable pK_a-values

A series of novel pH sensitive rosamine dyes with tunable pK_a values was obtained in overall yields of up to 30% by the condensation of differently substituted benzaldehydes with 3-aminophenol derivatives (see Fig. 2A and B). The condensation was carried out using propionic acid and a catalytic amount of *p*-toluenesulfonic acid (*p*-TsOH), followed by oxidation with chloranil. The rosamine scaffold was derived from rhodamine B (RhB), rhodamine 101 (Rh101), and tetramethylrhodamine (TMR), which differ in their substitution pattern at the xanthene ring systems and thus, in their spectroscopic properties. By using differently brominated *ortho*- and *para*-hydroxyphenyl as pH-sensitive moiety, a set of pH-responsive rosamines (**1a-2d**) was obtained with pK_a values varying from 4 to 9 (Fig. 2B). Also, a pH-inert reference dye **3** was synthesized consisting of a xanthene and unsubstituted phenolic unit.

3.2 Structure/property relationship of the rosamine dyes

Subsequently, the influence of the substitution pattern of the phenolic subunits and the nitrogen atoms at the xanthene core on the pH-dependent spectroscopic behavior of the dyes was examined. As previously stated, the former introduces the desired pH-sensitivity and tunability of the pK_a value, while the latter determines the photophysical properties of the dyes such as the spectral position of the absorption and emission

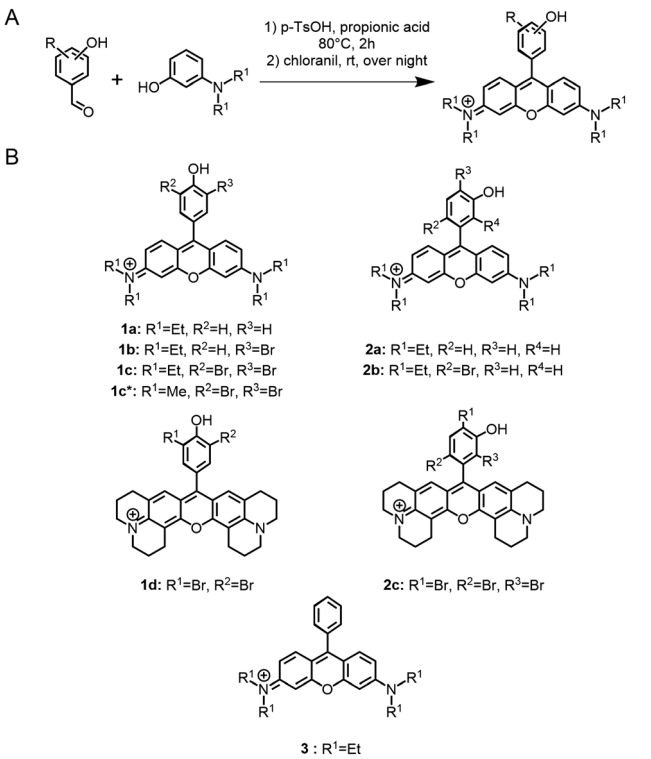

Fig. 2 (A) General synthetic route and (B) chemical structures of the synthesized pH-sensitive fluorescent rosamine probes.

Table 1 Overview of the photophysical properties of the synthesized rosamine dyes

Dye	ε (λ_{max}) (MeOH) [M^{-1} cm^{-1}]	$\lambda_{abs\text{-}ON}$ (MeOH) [nm]	λ_{em} (MeOH) [nm]	Φ_{fl} (EtOH)(abs.) [%]	τ_{fl} (MeOH)[a] [ns]	pK_a[b] (Em)
1a	81 000	551	570	35	1.73	8.99
1b	93 000	556	577	34	1.66	7.37
1c	86 000	561	580	27	1.56	5.51
1c*	58 000	555	578	32	1.98	5.54
1d	70 000	582	600	70	4.13	5.87
2a	65 500	553	576	35	1.72	9.42
2b	53 000	565	580	33	1.64	8.71
2c	57 000	600	620	56	4.44	5.14
3	76 000	555	575	32	1.65	n. a.

[a] Mono exponential fit (global analysis f_i (%) = 100.0). [b] In H_2O/MeOH 2 : 1 vol%, 25 mM buffered solution).

maxima ($\lambda_{abs(max)}$, $\lambda_{em(max)}$), the fluorescence quantum yields (ϕ), and the fluorescence lifetimes (τ). An overview of the spectroscopic properties of the new rosamine compounds in methanol is provided in Table 1. The molar absorption coefficients ε of the rosamines are in the order of 38 000–90 000 M^{-1} cm^{-1} and the ϕ values amount to 30–80% in methanol. Fig. 3A shows a comparison of the absorption and emission spectra of compounds bearing alkyl groups or fully rigidized xanthene scaffolds. For the alkyl substituted compounds, similar absorption and emission spectra with absorption and emission maxima at 555 nm and 580 nm are observed. The absorption and emission spectra of the compounds with a fused xanthene nitrogen are bathochromically shifted by 20 nm yielding absorption and emission maxima at 583 nm and 602 nm, respectively. This is ascribed to the enhanced delocalization of the electron density of the nitrogen electron pairs favored by the restricted rotation around the C–N bonds caused by the fused rings of compound **1d**. The influence of the halogen substituents on the phenyl ring is illustrated in Fig. 3B. This figure compares the absorption and emission spectra of the non-halogenated rosamine reference dye **3** with those of the *para*-hydroxy substituted non-, mono- and di-brominated rosamine dyes **1a**, **1b**, and **1c**. Apparently, introducing a hydroxy group on the phenyl ring does not affect the rosamine absorption and emission spectra, while each bromine atom induces a red shift of 5 nm of the absorption and emission maxima. The absorption maximum of **3** at 551 nm is shifted to 556 nm for **1a** and to 561 nm for **1b** and **1c** and the emission maxima from 572 nm to 577 nm and 583 nm, respectively. Similar shifts in absorption and emission results also for the *meta*-hydroxy substituted rosamine derivatives **2a–c** in dependence of the degree of bromination of the phenyl moiety (see Table 1). The very similar spectral properties of **1a–c** and **2a–b** as well as **1d** and **2c** indicate more or less complete electronic decoupling of the rosamine chromophore and the phenyl moiety inducing pH-sensitivity. Deprotonation of the hydroxyl group of the pH-responsive rosamines leads to a hypsochromic shift in absorption of about 10 nm whereas the absorption spectrum of the reference dye **3** remains unaffected by pH (see ESI,† Fig. S2–S10). Such a protonation-induced hypsochromic shift of the main absorption band is a consequence of the charge localization originating from an aromatic destabilization in the molecules and was observed for different pH sensitive fluorophores.[46–49] Consequently, these changes are attributed to an equilibrium between the cationic form

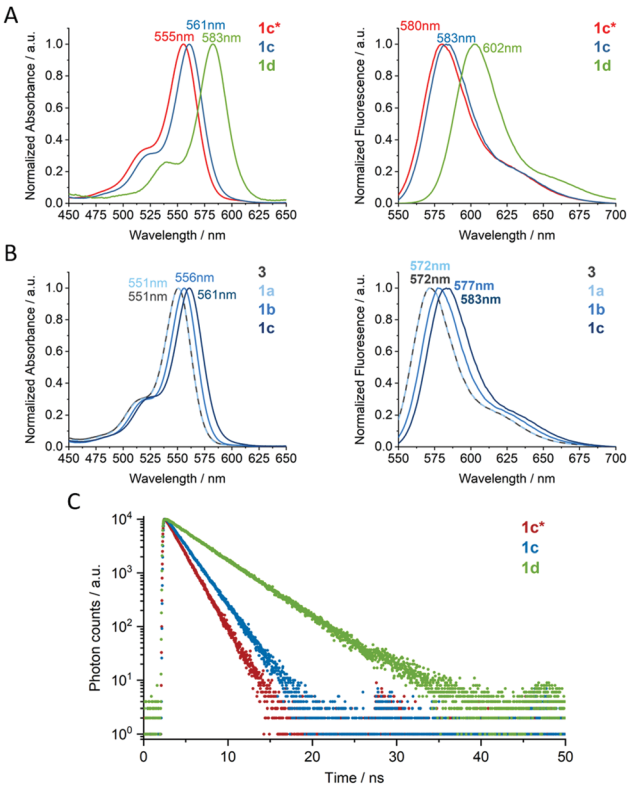

Fig. 3 Influence of (A) the xanthene moiety and (B) the bromination degree on the spectral position of the absorption and emission maxima. (C) Luminescence decay kinetics of different xanthene moieties.

(protonated hydroxyl group) and zwitterionic form (deprotonated hydroxyl group) of the rosamines introduced by deprotonation of the hydroxylic group and the increased electron density (enhanced electron donor strength) – of the negatively charged hydroxylic group located in the immediate proximity of the rhodamine core. The ϕ values of the rosamines are reduced by 30% compared to their parent rhodamine dyes (Φ_{EtOH}(RhB) = 69%, Φ_{EtOH}(TMR) = 68%, Φ_{EtOH}(Rh101) = 96% at 25 °C).[50] (see Table 1) This diminution in ϕ is ascribed to the absence of the carboxylic group in 2′ position, which permits rotation of the phenolic moiety, thereby opening further non-emissive relaxation pathways. A similar behavior was also observed by Mottram *et al.*[51] The rosamine dyes reveal mono-exponential fluorescence decay kinetics in methanol with τ_f values in the nanosecond (ns) range. The rosamine dyes **1d** and **2c** with

fused xanthene nitrogen atoms possess the longest lifetimes of around 4 ns, whereas the rosamines bearing *N*-alkyl groups have fluorescence lifetimes of less than two ns (Fig. 3C). Bromination of the phenol group is accompanied by a diminution in τ_f as reflected, *e.g.* by a comparison of dye **1c** and non-brominated **1a** (see ESI,† Fig. S19). This trend is ascribed to the heavy-atom effect of bromine. Finally, the pH dependence of the fluorescence decay kinetics of the pH-sensitive rosamine dyes was examined. Therefore, the fluorescence decay curves were measured at selected pH values exemplary for dyes **1c** and **1d** (see ESI,† Fig. S23). The results indicate that no significant changes in the decay kinetics and fluorescence lifetimes of the dyes occur upon deprotonation.

pH sensitivity of the rosamine fluorescence. All rosamine dyes bearing a phenolic substituent are non-fluorescent in the unprotonated form due to PET-induced fluorescence quenching. Upon protonation, they reveal an efficient and very fast recovery of their fluorescence, accompanied by minimal spectral shifts in absorption as exemplary shown for dye **1b** in Fig. 4A. This enables fluorometric pH sensing. The fact that the fluorescence of reference compound **3** lacking a hydroxylic group is not affected by pH (see ESI,† Fig. S2) underlines the need for this deprotonable functionality to induce PET-related pH-control of the rosamine fluorescence. The amine groups of the xanthene core are obviously not involved in this sensing mechanism.

Moreover, as shown in Fig. 4B, we could successfully expand the concept of halogenating phenolic subunits to tune the pK_a of fluorescent probes utilized for different classes of fluorophores such as BODIPY dyes[21,22] to rosamine dyes. Stepwise bromination of the phenolic aryl moiety in position 9 of the xanthene core clearly provides substitution pattern control of the pK_a of this dye class with the degree of halogenation strongly influencing the acidity of the pH-sensitive hydroxy group due to its electron withdrawing effect. The results of the fluorometric pH titration experiments of the rosamine dyes are shown in the ESI† (Fig. S3–S10) and the pH titration curves used to derive the pK_a values are summarized in Fig. 4B. Unsubstituted compounds **2a** and **1a** exhibit the most basic pK_a values of 9.42 and 8.99, respectively. Monobromination lowers the pK_a values to 8.71 for **2b** and to 7.37 for **1b**. This demonstrates that substitution in *ortho*-position to the hydroxylic group (in the case of **1b**) has a stronger influence on the pK_a value than halogenation in *meta*-position (for **2b**). Further halogenation leads to more acidic pK_a values of 5.51 for the di-brominated compound **1c**. The lowest pK_a value of 5.14 is observed for the tri-brominated compound **2c**. While halogenation of the subunits plays an important role for the tuning of the pK_a value, a comparison of compounds **1c**, **1c***, and **1d** with different substitution pattern of the xanthene core, which exhibit pK_a values of 5.51, 5.54, and 5.87, respectively, shows that the substitution pattern of the xanthene core barely affects the pK_a value of the sensor dye.

Subsequently, the reversibility of the PET-triggered ON/OFF-switching of the rosamine fluorescence was investigated that accompanies the protonation/deprotonation of the hydroxyl group. Therefore, the pH of the dyes solutions was reversibly changed from pH of 2 to 10 in 10–12 cycles. As shown in the ESI,† in Fig. S12 and S13, all dyes reveal an excellent reversibility of their fluorescence with their initial fluorescence intensity at a pH of 2 being completely restored even after 12 deprotonation/protonation cycles. The observed slight decrease in fluorescence intensity is attributed to dilution effects and not to a loss in reversibility.

As some rhodamine dyes show a temperature sensitive fluorescence intensity, we also performed temperature dependent studies with the differently substituted rosamine dyes to clarify whether the derived pK_a values are temperature- dependent. Such a temperature dependence could hamper their suitability for pH-sensing. Representatively, the pK_a value of compound **1c** was determined at 20 °C and 40 °C. The obtained values of 5.50 and 5.48 for 20 °C and 40 °C underline the temperature independence of the pH-sensing behavior (see ESI,† Fig. S11).

Temperature sensitivity of the rosamine dyes

As the substitution pattern, of the xanthene scaffold of the parent rhodamine dyes, *i.e.*, the degree of rigidity of the amino substituents can introduce a temperature dependence of the fluorescence,[44,52–54] the influence of temperature on fluorescence intensity was investigated for selected rosamine dyes. Our rosamine dyes can be classified into four groups with respect to their structural pattern, *i.e.*, the substitution pattern of the amino groups at the xanthene core and the phenolic moiety. This includes the following classes: (i) rigid-rigid (rigidized amino groups on the xanthene core and hindered rotation of the phenolic subunit (**2c**)), (ii) free-rigid (freely rotatable amino groups on the xanthene core and

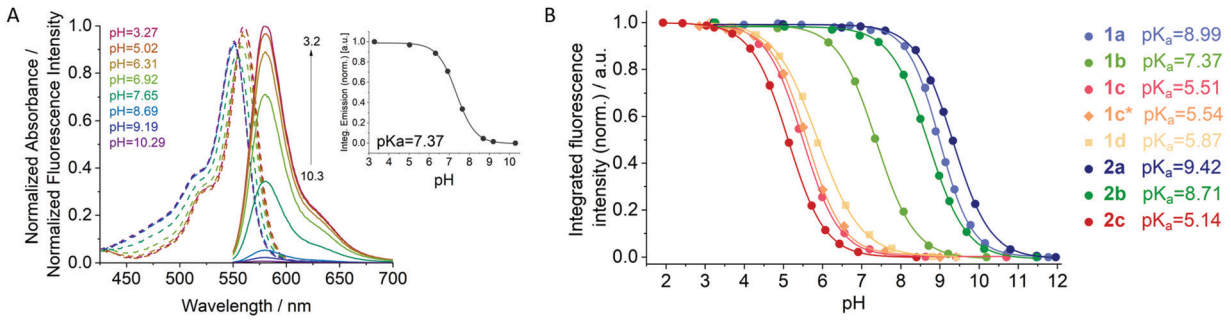

Fig. 4 (A) pH-dependent normalized absorption (dashed lines) and emission (solid lines) spectra of **1b** in a mixture of methanol-aqueous buffer solution (λ_{ex} = 540 nm). The insert shows a typical pH titration curve in the insert; (B) pH-titration curves (dose response equation fit) of all synthesized dyes illustrating the broad pH range covered by the novel rosamine dyes.

hindered rotation of the phenolic subunit (**2b**)), (iii) rigid-free (rigidized amino groups on the xanthene core and free rotation of the phenolic subunit (**1d**)), and (iv) free-free (freely rotatable amino groups on the xanthene core and non-hindered rotation of the phenolic subunit (**1c**)). Subsequently, we studied the temperature dependence of the fluorescence of representative rosamine dyes from each structural class. The changes of the integrated fluorescence intensities of the studied dyes in dependence of the temperature in a temperature interval from 10 °C to 50 °C are highlighted in Fig. 5. The corresponding absorption and emission spectra of the four dyes are provided in the ESI† (see Fig. S14–S17). For a better comparison of the different rosamines, the fluorescence intensities were normalized to the fluorescence intensity at 10 °C and a linear fit of the temperature-dependent changes using the least-mean-squares method was applied. This yielded fluorescence intensity changes of approximately −1.59%, −1.57%, −0.49%, and −0.15% per °C for **1c**, **2b**, **1d**, and **2c**, respectively. The absorption spectra of the dyes display only a small temperature-dependent decrease of the absorption maximum by 0.5–1%. Dye **2c**, representing the rigid–rigid class (i) reveals a quasi-temperature insensitive fluorescence. This is ascribed to the rigidization of the xanthene anilines as fused cyclic rings and the sterically restricted rotation of the phenolic subunit induced by substitution in positions 2′and 6′. However, reducing the overall rigidity of the dyes by either reducing the rigidity of the amine scaffold at the xanthene core (class i) or enabling a rotation of the phenolic PET-subunit (class iii) results in an enhanced temperature sensitivity favored by the thereby opened non-radiative relaxation pathways. For example, for dye **1d**, representing (class iii), a slight decrease in fluorescence intensity with increasing temperature is accordingly observed. Dyes **2b** and **1c** (classes (ii) and (iv)) reveal a similar, yet more pronounced temperature sensitivity. This behavior is ascribed to the free rotation of the alkylated amines on the xanthene core, enabling an electron transfer from the amino groups to the xanthene ring, that leads to a fast non-radiative deactivation to the ground state ascribed to a twisted intermolecular charge-transfer (TICT) process.[19] Notably, the degree of rotational hindrance of the phenolic group has only a negligible effect.

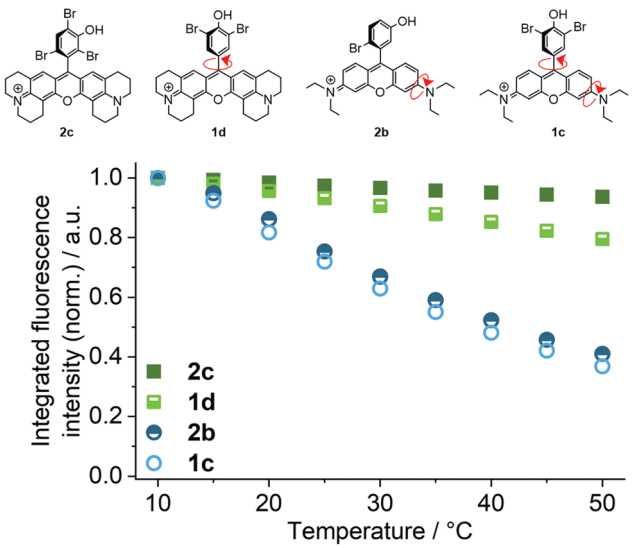

Fig. 5 Integrated fluorescence intensity of dyes **1c**, **1d**, **2b** and **2c** as a function of temperature.

4 Conclusions

In summary, we developed a simple and efficient strategy for the synthesis of a series of moderately to strongly fluorescent rosamine dyes with pK_a values tunable between 5.1 to 9.5 that can be utilized for pH sensing in the pH window of 4 to 10. The rational design of these sensor molecules relies on a phenolic subunit electronically decoupled from the xanthene core. The latter determines the spectral features of the fluorescent probes while the protonation state of the former controls the dye's fluorescence *via* an intramolecular photoinduced electron transfer (PET). Protonation of the phenol group inhibits the fluorescence quenching PET, leading to a pH dependent switching ON of the rosamine fluorescence. Tuning of the pK_a values of these pH-sensitive rosamines could be achieved by systematically introducing electron withdrawing groups like bromine atoms to the phenolic PET-inducing subunit. This strategy has been previously utilized by us also for a set of BODIPY dyes.[22] Moreover, a temperature-dependent fluorescence response of the rosamines can be promoted or suppressed in dependence of the rigidity of the dye scaffold, as reported for the rhodamine parent dyes. Thereby, rosamine dyes with a rigid scaffold as dye **2c** and thus suppressed temperature sensitivity, are excellent candidates for pH sensors. In addition, our findings provide new insights into a class of molecules that are responsive to two parameters, here pH and temperature, by different mechanisms. This could be interesting in the future, *e.g.* for the design of logic gates.[55,56]

Currently, we are equipping our pH-responsive rosamines with a linker group on the phenol moiety. This will enable the facile coupling of these promising fluorophores to biomolecules such as antibodies or nanoparticles bearing reactive surface groups to construct pH-responsive bioconjugates and nanosensors for bioimaging applications.

Conflicts of interest

There are no conflicts to declare.

Acknowledgements

This work was funded by the German Research Council DFG (grant SCHA 1009/17-1) and Bundesanstalt für Materialforschung und -prüfung (BAM). NMR and MS measurements were performed at FU Berlin.

References

1 J. Wu, W. Liu, J. Ge, H. Zhang and P. Wang, *Chem. Soc. Rev.*, 2011, **40**, 3483–3495.
2 T. Ueno and T. Nagano, *Nat. Methods*, 2011, **8**, 642–645.

3 H. Zhu, J. Fan, J. Du and X. Peng, *Acc. Chem. Res.*, 2016, **49**, 2115–2126.
4 K. Kikuchi, *Chem. Soc. Rev.*, 2010, **39**, 2048–2053.
5 T. Terai and T. Nagano, *Pflugers Arch*, 2013, **465**, 347–359.
6 Y. Yang, Q. Zhao, W. Feng and F. Li, *Chem. Rev.*, 2013, **113**, 192–270.
7 K. Kaur, R. Saini, A. Kumar, V. Luxami, N. Kaur, P. Singh and S. Kumar, *Coord. Chem. Rev.*, 2012, **256**, 1992–2028.
8 D. T. Quang and J. S. Kim, *Chem. Rev.*, 2010, **110**, 6280–6301.
9 M. J. Culzoni, A. Muñoz de la Peña, A. Machuca, H. C. Goicoechea and R. Babiano, *Anal. Methods*, 2013, **5**, 30–49.
10 S. Suganya, S. Naha and S. Velmathi, *ChemistrySelect*, 2018, **3**, 7231–7268.
11 J. Han and K. Burgess, *Chem. Rev.*, 2010, **110**, 2709–2728.
12 D. Wencel, T. Abel and C. McDonagh, *Anal. Chem.*, 2014, **86**, 15–29.
13 J.-T. Hou, W. X. Ren, K. Li, J. Seo, A. Sharma, X.-Q. Yu and J. S. Kim, *Chem. Soc. Rev.*, 2017, **46**, 2076–2090.
14 S. Wen, L. Xiaohua and M. Huimin, *Methods Appl. Fluoresc.*, 2014, **2**, 042001.
15 A. Steinegger, O. S. Wolfbeis and S. M. Borisov, *Chem. Rev.*, 2020, **120**, 12357–12489.
16 Y. Q. Li, J. L. Bricks, U. Resch-Genger, M. Spieles and W. Rettig, *J. Phys. Chem. A*, 2006, **110**, 10972–10984.
17 K. Rurack and U. Resch-Genger, *Chem. Soc. Rev.*, 2002, **31**, 116–127.
18 Y. Fu and N. S. Finney, *RSC Adv.*, 2018, **8**, 29051–29061.
19 Z. R. Grabowski, K. Rotkiewicz and W. Rettig, *Chem. Rev.*, 2003, **103**, 3899–4032.
20 K. M. K. S. Ha Na Kim and Juyoung Yoon, *Tetrahedron Lett.*, 2011, **52**, 2340–2343.
21 J. Qi, D. Liu, X. Liu, S. Guan, F. Shi, H. Chang, H. He and G. Yang, *Anal. Chem.*, 2015, **87**, 5897–5904.
22 S. Radunz, H. R. Tschiche, D. Moldenhauer and U. Resch-Genger, *Sens. Actuators, B*, 2017, **251**, 490–494.
23 R. Gotor, P. Ashokkumar, M. Hecht, K. Keil and K. Rurack, *Anal. Chem.*, 2017, **89**, 8437–8444.
24 Y. S. Marfin, M. V. Shipalova, V. O. Kurzin, K. V. Ksenofontova, A. V. Solomonov and E. V. Rumyantsev, *J. Fluoresc.*, 2016, **26**, 2105–2112.
25 C. Staudinger, J. Breininger, I. Klimant and S. M. Borisov, *Analyst*, 2019, **144**, 2393–2402.
26 R. Zhang, F. Yan, Y. Huang, D. Kong, Q. Ye, J. Xu and L. Chen, *RSC Adv.*, 2016, **6**, 50732–50760.
27 L. D. Lavis and R. T. Raines, *ACS Chem. Biol.*, 2008, **3**, 142–155.
28 K. Othmer, *Encyclopedia of Chemical Technology*, 2000, pp. 1–19, DOI: 10.1002/0471238961.2401142023090708.a01.pub2.
29 X. Chen, T. Pradhan, F. Wang, J. S. Kim and J. Yoon, *Chem. Rev.*, 2012, **112**, 1910–1956.
30 H. Zheng, X.-Q. Zhan, Q.-N. Bian and X.-J. Zhang, *Chem. Commun.*, 2013, **49**, 429–447.
31 S. Ma, Y. Wang, M. She, S. Wang, Z. Yang, P. Liu, S. Zhang and J. Li, *Rev. Anal. Chem.*, 2017, **36**, 20160024.
32 W. Zhang, B. Tang, X. Liu, Y. Liu, K. Xu, J. Ma, L. Tong and G. Yang, *Analyst*, 2009, **134**, 367–371.
33 Q. A. Best, R. Xu, M. E. McCarroll, L. Wang and D. J. Dyer, *Org. Lett.*, 2010, **12**, 3219–3221.
34 L. Yuan, W. Lin and Y. Feng, *Org. Biomol. Chem.*, 2011, **9**, 1723–1726.
35 Z. Li, S. Wu, J. Han and S. Han, *Analyst*, 2011, **136**, 3698–3706.
36 M. Tian, X. Peng, J. Fan, J. Wang and S. Sun, *Dyes Pigm.*, 2012, **95**, 112–115.
37 A. Bender, Z. R. Woydziak, L. Fu, M. Branden, Z. Zhou, B. D. Ackley and B. R. Peterson, *ACS Chem. Biol.*, 2013, **8**, 636–642.
38 H.-S. Lv, S.-Y. Huang, Y. Xu, X. Dai, J.-Y. Miao and B.-X. Zhao, *Bioorg. Med. Chem. Lett.*, 2014, **24**, 535–538.
39 W. L. Czaplyski, G. E. Purnell, C. A. Roberts, R. M. Allred and E. J. Harbron, *Org. Biomol. Chem.*, 2014, **12**, 526–533.
40 S. G. Stratton, G. H. Taumoefolau, G. E. Purnell, M. Rasooly, W. L. Czaplyski and E. J. Harbron, *Chem. – Eur. J.*, 2017, **23**, 14064–14072.
41 H. N. Kim, M. H. Lee, H. J. Kim, J. S. Kim and J. Yoon, *Chem. Soc. Rev.*, 2008, **37**, 1465–1472.
42 S. Uchiyama, A. Prasanna de Silva and K. Iwai, *J. Chem. Educ.*, 2006, **83**, 720.
43 K. Kemnitz and K. Yoshihara, *J. Phys. Chem.*, 1991, **95**, 6095–6104.
44 D. Moreau, C. Lefort, R. Burke, P. Leveque and R. P. O'Connor, *Biomed. Opt. Express*, 2015, **6**, 4105–4117.
45 M. Gemma, P. Irene Pérez, F. Nicholas, G. D. Peter, R. B. Olivier and A. Manfred, *Methods Appl. Fluoresc.*, 2015, **3**, 045002.
46 D. Aigner, S. M. Borisov, F. J. Orriach Fernández, J. F. Fernández Sánchez, R. Saf and I. Klimant, *Talanta*, 2012, **99**, 194–201.
47 R. Sun, X.-D. Liu, Z. Xun, J.-M. Lu, Y.-J. Xu and J.-F. Ge, *Sens. Actuators, B*, 2014, **201**, 426–432.
48 G. Despras, A. I. Zamaleeva, L. Dardevet, C. Tisseyre, J. G. Magalhaes, C. Garner, M. De Waard, S. Amigorena, A. Feltz, J.-M. Mallet and M. Collot, *Chem. Sci.*, 2015, **6**, 5928–5937.
49 Y. Chen, D. Qi, L. Zhao, W. Cao, C. Huang and J. Jiang, *Chem. – Eur. J.*, 2013, **19**, 7342–7347.
50 R. F. Kubin and A. N. Fletcher, *J. Lumin.*, 1982, **27**, 455–462.
51 L. F. Mottram, S. Forbes, B. D. Ackley and B. R. Peterson, *Beilstein J. Org. Chem.*, 2012, **8**, 2156–2165.
52 V. M. Chauhan, R. H. Hopper, S. Z. Ali, E. M. King, F. Udrea, C. H. Oxley and J. W. Aylott, *Sens. Actuators, B*, 2014, **192**, 126–133.
53 S. Claucherty and H. Sakaue, *Sens. Actuators, B*, 2017, **240**, 956–961.
54 Y. Wu, J. Liu, J. Ma, Y. Liu, Y. Wang and D. Wu, *ACS Appl. Mater. Interfaces*, 2016, **8**, 14396–14405.
55 A. Diacono, M. C. Aquilina, A. Calleja, G. Agius, G. Gauci, K. Szaciłowski and D. C. Magri, *Org. Biomol. Chem.*, 2020, **18**, 4773–4782.
56 S. Uchiyama, N. Kawai, A. P. de Silva and K. Iwai, *J. Am. Chem. Soc.*, 2004, **126**, 3032–3033.

